Novel Disordering Mechanism in Ferromagnetic Systems with Competing Interactions

Juan Carlos Andresen,[1] Creighton K. Thomas,[2,*] Helmut G. Katzgraber,[2,3,1] and Moshe Schechter[4]

[1]*Theoretische Physik, ETH Zurich, CH-8093 Zurich, Switzerland*
[2]*Department of Physics and Astronomy, Texas A&M University, College Station, Texas 77843-4242, USA*
[3]*Materials Science and Engineering Program, Texas A&M University, College Station, TX 77843, USA*
[4]*Department of Physics, Ben Gurion University, Beer Sheva 84105, Israel*

(Dated: May 29, 2018)

Ferromagnetic Ising systems with competing interactions are considered in the presence of a random field. We find that in three space dimensions the ferromagnetic phase is disordered by a random field which is considerably smaller than the typical interaction strength between the spins. This is the result of a novel disordering mechanism triggered by an underlying spin-glass phase. Calculations for the specific case of the long-range dipolar $\mathrm{LiHo_xY_{1-x}F_4}$ compound suggest that the above mechanism is responsible for the peculiar dependence of the critical temperature on the strength of the random field and the broadening of the susceptibility peaks as temperature is decreased, as found in recent experiments by Silevitch *et al*. [Nature (London) **448**, 567 (2007)]. Our results thus emphasize the need to go beyond the standard Imry-Ma argument when studying general random-field systems.

PACS numbers: 75.50.Lk, 75.40.Mg, 05.50.+q, 64.60.-i

Introduction.— The random-field Ising model (RFIM) plays a central role in the study of disordered systems and has been applied to problems across disciplines ranging from disordered magnets to random pinning of polymers, as well as water seepage in porous media.

At and below the lower critical dimension $d_\ell = 2$, the ferromagnetic (FM) phase is unstable to an infinitesimal random field (RF) [1, 2]. At higher space dimensions the disordering of the FM phase requires the RF strength h to be of the order of the spin-spin interaction strength J. Yet, the effect of the RF on the transition between the FM and paramagnetic (PM) phases—for systems with both short-range and dipolar interactions—has been source of vast experimental and theoretical scrutiny [3–5]. Over the past three decades the RFIM has been studied experimentally via dilute antiferromagnets in a field (DAFF) [6], as both the RFIM and the DAFF seem to share the same universality class. More recently it has been shown that in anisotropic dipolar magnets the RFIM can be realized in the FM phase: By applying a transverse field to a dilute dipolar ferromagnet, such as $\mathrm{LiHo_xY_{1-x}F_4}$, one transforms the spatial disorder to a longitudinal *effective* RF [7–9]. This opens the doors for advancing our understanding of the RF problem [10], as well as new applications, such as tunable domain-wall pinning [11] in magnetic materials.

Silevitch *et al.* recently studied the FM-to-PM transition in the presence of RFs in $\mathrm{LiHo_xY_{1-x}F_4}$ [12]. Remarkably, they found that T_c depends linearly on the transverse field (and thus on h [7, 9]) and that the susceptibility peak diminishes and broadens as temperature decreases. In $\mathrm{Mn_{12}-ac}$, which is a realization of the RFIM with all FM interactions, a strong suppression of T_c as a function of h was found as well [13], but with what appears to be a quite different functional dependence at small h.

Here we study the interplay between FM and spin-glass (SG) phases in a dipolar Ising model with competing interactions in the presence of a RF. We find a novel disordering mechanism of the FM phase when a RF is applied and the system is in close proximity (e.g., via dilution) to a SG phase. This disordering mechanism lies between the Imry-Ma and standard disordering mechanisms: The disordering of the FM phase occurs at a finite RF, which is considerably smaller than the typical spin-spin interaction, and the disordered phase [denoted henceforth as "quasi-SG" (QSG)] consists of not FM but glassy domains. At $T = 0$ we predict the existence of a FM-to-QSG transition and determine for $\mathrm{LiHo_xY_{1-x}F_4}$, analytically and numerically, the phase boundary as a function of the Ho concentration x and RF strength h. At finite temperature our theory agrees with experiments [12], suggesting that the existence of competing interactions and the proximity to the SG phase dictate the broadening of the susceptibility peaks at low temperature and the peculiar dependence of T_c on h. Our theoretical analysis of the SG phase follows the scaling approach of Fisher and Huse [14]—its validity supported by the agreement we find with our numerical results. The nature of the SG phase in a RF, however, is controversial [15–30], but of no concern here.

Theoretical analysis.— We first study $\mathrm{LiHo_xY_{1-x}F_4}$ at $T = 0$. For dilutions $x > x_c$ the system is FM, whereas for $x_0 < x < x_c$ the system is a SG. Below we show numerically that $x_c \approx 0.3$. To date, it is unclear if $x_0 > 0$ [31, 32]. For $x \approx x_c$ we define the energy per spin of the lowest FM state of the system as $f_{\mathrm{FM}}(x)$, and the lowest energy of the SG state as $f_{\mathrm{SG}}(x)$. Note that $f_{\mathrm{FM}}(x)$ is the ground-state energy of the FM phase when $x > x_c$ and $f_{\mathrm{SG}}(x)$ represents the ground-state energy of the SG phase for $x_0 < x < x_c$. At $x = x_c$ $f_{\mathrm{FM}}(x_c) = f_{\mathrm{SG}}(x_c)$, and for $x \approx x_c$, to first order in $x - x_c$, $f_{\mathrm{SG}}(x) - f_{\mathrm{FM}}(x) = \alpha(x - x_c) + \ldots$. We consider the FM phase for $x > x_c$ in an applied RF of mean zero and standard deviation h. For small h, the FM state in three dimensions cannot gain energy from the field, because domain flips are not energetically favorable. However, for spin glasses the lower critical (Imry-Ma) dimension is infinity [14]. In particular, in

3D the energy of the system can be lowered by flipping domains, creating a QSG phase with a finite correlation length. Thus, for $x \sim x_c$ the energy of the SG state will become lower than the energy of the FM state at a finite RF, which is still considerably smaller than the typical spin-spin interaction J. More generally, any 3D Ising system with competing interactions having at zero RF a FM ground state and a SG state at a somewhat higher energy will be disordered through a transition to the QSG phase at a finite RF whose magnitude depends on the proximity to the SG phase and can be much smaller than J. Because in systems like $LiHo_xY_{1-x}F_4$ the effective RFs are a result of quantum fluctuations [7, 33], this phase transition is a particular case of a quantum phase transition where the quantum fluctuations of the spins are small, involving only the spin's ground and first excited states [34], but where the *collective effect* of all spins is strong enough to drive the transition.

The value of the critical RF can be estimated using the short-range Hamiltonian [35] in a RF $H_{\rm EA} = -\sum_{\langle ij\rangle} J_{ij}S_iS_j + \sum_i h_iS_i$. J_{ij} represent nearest-neighbor Gaussian random bonds between spins S_i with zero mean and standard deviation J, and h_i are Gaussian RFs of average strength h [36]. The SG ground state is unstable to an infinitesimal RF, creating domains of typical size $(J/h)^{1/(3/2-\theta)}$ ($\theta \approx 0.19$) [37]. The energy reduction per spin due to the RF is thus $f(h) = h(J/h)^{(-3/2)/(3/2-\theta)}$. The total energy reduction per spin is of the same order, because the energy cost to flip domains is much smaller. Considering now a FM system with competing interactions, e.g., $LiHo_xY_{1-x}F_4$ at $x > x_c$ where at $h = 0$ the system is FM with $f_{\rm SG} > f_{\rm FM}$, the critical field $h_c(x)$ can be computed from $f(h = h_c) = f_{\rm SG} - f_{\rm FM}$, i.e., $f(h = h_c) = \alpha(x - x_c)$. One obtains

$$h_c(x) = \alpha'(J)(x - x_c)^{(3/2-\theta)/(3-\theta)}, \qquad (1)$$

where $\alpha'(J) = \alpha^{(3/2-\theta)/(3-\theta)}J^{(3/2)/(3-\theta)}$; see Fig. 1. For $h > h_c(x)$ there are finite domains within which glassy order persists. The domain size decreases with increasing field, where at $h \approx J$ the system resembles a paramagnet. As $x \to x_c$, the disordering field approaches zero. For large $x - x_c$ and $h \approx J$ there is a crossover to the standard behavior where the disordering is a result of single-spin energy minimization; i.e., the intermediate QSG regime disappears.

We now consider finite temperatures and analyze the dependence of the FM T_c (at $x > x_c$) on the effective RF. Let us denote the lowest free energies per spin of the FM phase (ordered for $T < T_{\rm FM}$, disordered for $T > T_{\rm FM}$) and a competing disordered QSG phase as $F_{\rm FM}(x, T)$ and $F_{\rm QSG}(x, T)$, respectively. Because the entropy of the QSG phase is dominated by regions at the boundaries between domains [14], the main effect of the RFs is to lower the QSG energy. Thus, $F_{\rm QSG}(x, T) - F_{\rm FM}(x, T) = -A(T - T_{\rm FM}) + B(x - x_c) - h/\xi_{\rm QSG}^{3/2}$ [here, for $h = 0$, $F_{\rm QSG}(x_c, T_c) = F_{\rm FM}(x_c, T_c)$]. For $h < h^* \equiv B(x - x_c)\xi^{3/2}$ and $T = T_{\rm FM}$ we obtain $F_{\rm QSG}(x, T) > F_{\rm FM}(x, T)$, and the transition occurs between an ordered FM phase and a disordered PM phase dominated by FM fluctuations. However, for $h > h^*$ we obtain $T_c(h) - T_c(0) = A^{-1}\left[B(x - x_c) - h/\xi^{3/2}\right]$, where the FM phase is disordered by a PM phase dominated by fluctuations of domains having SG correlations over distance ξ. Thus, at $h = h^*$, $T_c(h)$ has a crossover from a roughly quadratic dependence on the RF (known for a ferromagnet in a RF [38]) to a linear dependence. This result is supported by our numerics.

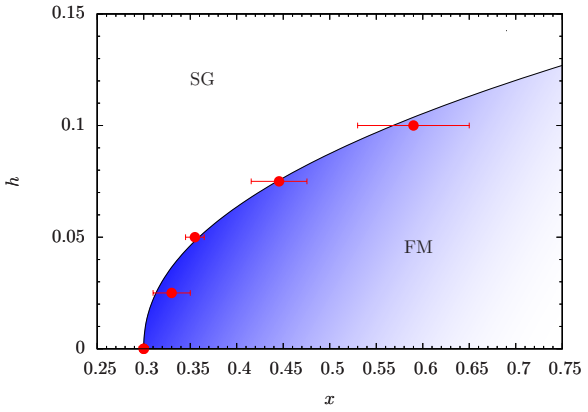

FIG. 1: (color online) Comparison of the zero-temperature numerical and analytical [Eq. (1)] h-x phase diagrams for the diluted dipolar Ising model [Eq. (2)]. $h_c(x) \sim (x - x_c)^{0.466}$, with $\theta \approx 0.19$ [37]. The analytical prediction agrees well with the numerical data (α' is a fitting parameter).

Comparing to the experiments in Ref. [12], our results are consistent with $T_c(h)$ being linear when $h \ll J$, with deviations from linearity as $h \to 0$. Note that in Ref. [12] $T_c(h)$ is linear down to the lowest RFs studied if one defines T_c by the asymptotic behavior of the susceptibility at high temperatures. However, if $T_c(h)$ is defined by the peak position of the susceptibility, deviations from linearity are observed at low fields [39].

Numerical details.— $LiHo_xY_{1-x}F_4$ at low temperatures and in an external transverse magnetic field is well described by [9, 40]

$$\mathcal{H} = \sum_{i\neq j} \frac{J_{ij}}{2}\epsilon_i\epsilon_j S_iS_j + \frac{J_{\rm ex}}{2}\sum_{\langle i,j\rangle} \epsilon_i\epsilon_j S_iS_j + \sum_i h_i\epsilon_i S_i\,. \quad (2)$$

Here $\epsilon_i = \{0, 1\}$ is the occupation of the magnetic Ho^{3+} ions on a tetragonal lattice (lattice constants $a = b = 5.175$Å and $c = 10.75$Å) with four ions per unit cell [41, 42], $S_i \in \{\pm 1\}$, h_i represent Gaussian RFs with zero mean and standard deviation h, where h is measured in $[K]$. The magnetostatic dipolar coupling J_{ij} between two Ho^{3+} ions is given by: $J_{ij} = D(r_{ij}^2 - 3z_{ij}^2)/r_{ij}^5$, where $r_{ij} = |\mathbf{r}_i - \mathbf{r}_j|$, $\mathbf{r}_i$ is the position of the ith Ho^{3+} ion and $z_{ij} = (\mathbf{r}_i - \mathbf{r}_j)\cdot\hat{z}$ is the component parallel to the easy axis. $D/a^3 = 0.214$K [43] and the nearest-neighbor exchange is $J_{\rm ex} = 0.12$K [41, 44]. We use periodic boundary conditions with Ewald sums [42, 45]. At zero field and no dilution, we find $T_c = 1.5316(2)$K, in agreement with experimental results where $T_c = 1.530(5)$K [46].

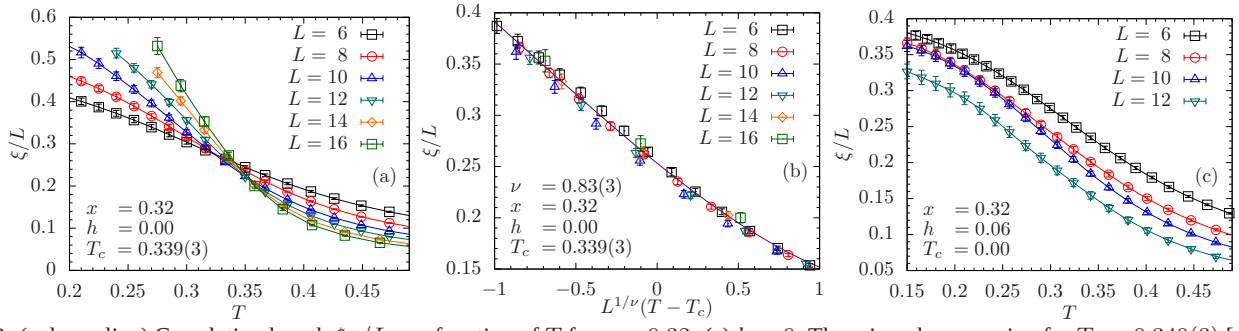

FIG. 2: (color online) Correlation length ξ_L/L as a function of T for $x = 0.32$. (a) $h = 0$. There is a clear crossing for $T_c = 0.340(3)$ [44] for different system sizes L. (b) Scaling of the data for $h = 0$. The solid line represents the optimal scaling function (polynomial approximation). (c) $h = 0.06$. There is no transition.

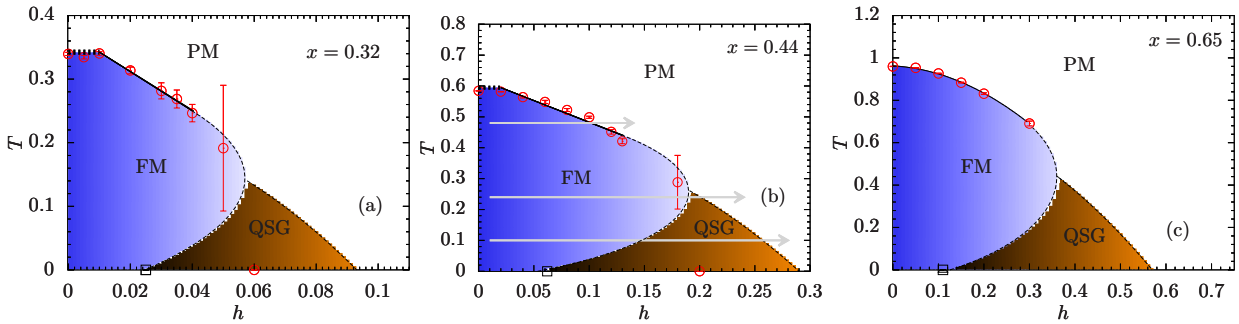

FIG. 3: (color online) T-h phase diagram of $LiHo_xY_{1-x}F_4$ for different concentrations x. Circles represent data from finite-temperature simulations, squares data from zero-temperature simulations (see Fig. 1). (a) $x = 0.32$. (b) $x = 0.44$ (dilution used in the experiments of Ref. [12]). Horizontal lines denote lines of constant temperature and varying h, as done experimentally [12] in susceptibility measurements. The top line has a direct FM-PM transition. The bottom two lines represent paths crossing the QSG phase where a broadening of the susceptibility peak and its diminishing with the enhancement of the RF at the crossover to the PM phase as temperature is decreased occur. (c) $x = 0.65$. In all panels, dotted line segments represent the conjectured phase boundary.

For the zero-temperature simulations (Fig. 1) we use jaded extremal optimization [47, 48]. Here, $\tau = 1.6$, 1.8 and 2 with an aging parameter $\Gamma = 0.05$ for at least 2^{26} steps. Ground states are found with high confidence for $L \leq 10$ and $h = 0$, and $L \leq 8$ with small $h \neq 0$. The phase boundary is identified via the Binder ratio $g = (1/2)(3 - \left[m^4\right]_{\rm av} / \left[m^2\right]^2_{\rm av})$, where $m = (1/N)\sum_i S_i$ ($N = 4xL^3$ is the number of spins and $[\cdots]_{\rm av}$ represents a disorder average. $g \sim \tilde{G}[L^{1/\nu}(x - x_c)]$ is a dimensionless function, allowing for the extraction of x_c and ν for a fixed h. Parameters are listed in the Supplementary Material, Table I [49].

At finite temperatures we use parallel tempering Monte Carlo [50]. Parameters are listed in Tables II, III and IV in the Supplementary Material [49]. To determine the transitions for a given h and x we measure [51]

$$\xi_L = \frac{1}{2\sin(k_{\rm min}/2)} \sqrt{\frac{[\langle m^2(\mathbf{0})\rangle_{\rm T}]_{\rm av}}{[\langle m^2(\mathbf{k}_{\rm min})\rangle_{\rm T}]_{\rm av}} - 1}\,, \qquad (3)$$

where $m(\mathbf{k}) = (1/N)\sum_{i=1} S_i \exp(i\mathbf{k}\cdot\mathbf{R}_i)$. Here $\langle\cdots\rangle_{\rm T}$ represents a thermal average, and $\mathbf{R}_i$ is the spatial location of the spin S_i, and $\mathbf{k}_{\rm min} = (2\pi/L, 0, 0)$. $\xi_L/L \sim \tilde{X}[L^{1/\nu}(T - T_c)]$; i.e., at the transition ($T = T_c$) the argument of $\tilde{X}$ is zero (up to scaling corrections) and hence independent of L [lines of different system sizes cross [Fig. 2(a)]]. If, however, the lines do not meet, no transition occurs [Fig. 2(c)]. To determine $T_c(h)$ we scale the data [Fig. 2(b)]. Using a bootstrapped Levenberg-Marquardt minimization [52] allows us to determine the critical parameters with statistical errors; see Table V of the Supplemental Material [49]. Note that for a given x the critical exponent ν increases with h.

Figure 1 shows the h-x phase diagram of $LiHo_xY_{1-x}F_4$ at zero temperature. We find excellent agreement with Eq. (1), using $\theta \approx 0.19$ [37], i.e., $h_c(x) \sim (x - x_c)^{0.466}$, and α' a fitting parameter (quality of fit $Q = 0.89$) [53]. Note, however, that good fits are also possible for $0.42 \lesssim z \lesssim 0.5$ with an optimal value of $z = 0.43(4)$ ($Q = 0.82$).

Figure 3 shows finite-temperature data for different x. Figure 3(a) shows $T_c(h)$ for $x = 0.32$, i.e., $x - x_c = 0.02$ small. Our results at finite T corroborate our theoretical model with $h^* \approx 0.01$, where for $h < h^*$, T_c is roughly independent of h (at such small fields the numerical resolution does not allow a distinction between a constant and a parabolic dependence) and for $h > h^*$, $T_c(h)$ decreases linearly. The FM phase fully disorders, at all temperatures, for $h \approx 0.055(5)$, a value slightly larger than found from the $T = 0$ simulations, yet much smaller than the interaction energy. Both the disordering of the FM phase at small fields and the linearity of $T_c(h)$ seem to persist up to $x = 0.44$ [Fig. 3(b)], the dilution used in Ref. [12], albeit with a less pronounced crossover at $h = h^*$.

For $x = 0.65$ [far from the SG phase, Fig. 3(c)] the behavior of $T_c(h)$ changes to a quadratic dependence for all $h < 0.3$, suggesting a standard FM-PM transition. Critical parameters are listed in the Supplemental Material, Table V [49].

Phase diagram: Reentrance and experiment.— Our analysis for *zero* RF suggests that the critical concentration $x_c = 0.3$ separating the FM and SG phases depends only slightly, if at all, on temperature. Reentrance to a SG phase is either missing or limited to a small concentration regime, in contrast to previous suggestions [54].

At the same time, our results at finite RF at both zero and finite temperature for all concentrations suggest that there is a range of RFs where the system shows reentrance to a frozen QSG phase at low temperatures [55]. The RF-temperature phase diagram is shown in Fig. 3. Note also that the PM phase is characterized by distinct correlations over the phase diagram: FM fluctuating domains close to the FM phase at $h < h^*$ [dashed line in Figs. 3(a) and 3(b)], and SG fluctuating domains close to the transition for $h > h^*$. This form of the phase diagram is strongly supported by, and provides an explanation for, the results of Ref. [12], Fig. 2. For $T > 0.3$K [inflection point in Fig. 3(b) above] there is a direct transition from the FM to the PM [top horizontal arrow in Fig. 3(b)], as is indeed marked experimentally by a sharp cusp in the magnetic susceptibility. For $T < 0.3$K, however, as the transverse field (and correspondingly the effective RF) is increased, the FM phase changes into a frozen QSG phase and only then to the PM phase [central horizontal arrow in Fig. 3(b)]. Experimentally, this effect is mirrored by a broad peak in the susceptibility at $T < 0.3$K, in good agreement with the inflection point we find at $x = 0.44$. As temperature is further reduced, the crossover between the frozen QSG phase and the PM phase occurs at a larger RF [bottom horizontal arrow in Fig. 3(b)], resulting in smaller glassy domains and the experimentally observed diminishing peak of the susceptibility [7, 56].

Conclusions.— We propose a novel disordering mechanism for 3D ferromagnets with competing interactions and an underlying spin-glass phase, resulting in a disordering field which is finite, yet can be much smaller than the interaction strength. We explain various aspects of the experiments of Ref. [12], including the peculiar linear dependence of T_c on the applied transverse field and the diminishing and broadening of the susceptibility peak with decreasing temperature. We further find that at smaller concentrations ($x = 0.32$, close to the spin-glass phase) the reduction of T_c with the RF becomes more pronounced. Our results strongly support the notion that it is the interplay between the competing interactions and the induced effective RF that dictate the behavior of the $\mathrm{LiHo_xY_{1-x}F_4}$ ferromagnet at low concentrations. Our analytical results are generic to FM systems with competing interactions. It would therefore be interesting to verify these results for other types of interactions and lattice structures[57].

H. G. K. acknowledges support from the SNF (Grant No. PP002-114713) and the NSF (Grant No. DMR-1151387). M.S. acknowledges support from the Marie Curie Grant No. PIRG-GA-2009-256313. The authors thank ETH Zurich for CPU time on the Brutus cluster and A. Aharony and D. Silevitch for useful discussions.

* Present address: Dept. of Materials Science and Engineering, Northwestern University, Evanston, Illinois 60208-3108, USA

[1] Y. Imry and S.-K. Ma, Phys. Rev. Lett. **35**, 1399 (1975).
[2] K. Binder, Z. Phys. B - Condensed Matter **50**, 343 (1983).
[3] T. Nattermann, J. Phys. A **21**, L645 (1988).
[4] D. P. Belanger, in *Spin Glasses and Random Fields*, edited by A. P. Young (World Scientific, Singapore, 1998), p. 251.
[5] T. Nattermann, in *Spin Glasses and Random Fields*, edited by A. P. Young (World Scientific, Singapore, 1998), p. 277.
[6] S. Fishman and A. Aharony, J. Phys. C **12**, L729 (1979).
[7] M. Schechter and N. Laflorencie, Phys. Rev. Lett. **97**, 137204 (2006).
[8] S. M. A. Tabei, M. J. P. Gingras, Y.-J. Kao, P. Stasiak, and J.-Y. Fortin, Phys. Rev. Lett. **97**, 237203 (2006).
[9] M. Schechter, Phys. Rev. B **77**, 020401(R) (2008).
[10] For a recent review and open problems see Ref. [58].
[11] D. M. Silevitch, G. Aeppli, and T. F. Rosenbaum, Proc. Natl. Acad. Sci. U.S.A. **107**, 2797 (2010).
[12] D. M. Silevitch, D. Bitko, J. Brooke, S. Ghosh, G. Aeppli, and T. F. Rosenbaum, Nature **448**, 567 (2007).
[13] B. Wen, P. Subedi, L. Bo, Y. Yeshurun, M. P. Sarachik, A. D. Kent, A. J. Millis, C. Lampropoulos, and G. Christou, Phys. Rev. B **82**, 014406 (2010).
[14] D. S. Fisher and D. A. Huse, Phys. Rev. B **38**, 386 (1988).
[15] R. N. Bhatt and A. P. Young, Phys. Rev. Lett. **54**, 924 (1985).
[16] J. C. Ciria, G. Parisi, F. Ritort, and J. J. Ruiz-Lorenzo, J. Phys. I France **3**, 2207 (1993).
[17] N. Kawashima and A. P. Young, Phys. Rev. B **53**, R484 (1996).
[18] A. Billoire and B. Coluzzi, Phys. Rev. E **68**, 026131 (2003).
[19] E. Marinari, C. Naitza, and F. Zuliani, J. Phys. A **31**, 6355 (1998).
[20] J. Houdayer and O. C. Martin, Phys. Rev. Lett. **82**, 4934 (1999).
[21] F. Krzakala, J. Houdayer, E. Marinari, O. C. Martin, and G. Parisi, Phys. Rev. Lett. **87**, 197204 (2001).
[22] H. Takayama and K. Hukushima, J. Phys. Soc. Jpn. **73**, 2077 (2004).
[23] A. P. Young and H. G. Katzgraber, Phys. Rev. Lett. **93**, 207203 (2004).
[24] H. G. Katzgraber and A. P. Young, Phys. Rev. B **72**, 184416 (2005).
[25] T. Jörg, H. G. Katzgraber, and F. Krzakala, Phys. Rev. Lett. **100**, 197202 (2008).
[26] H. G. Katzgraber, D. Larson, and A. P. Young, Phys. Rev. Lett. **102**, 177205 (2009).
[27] L. Leuzzi, G. Parisi, F. Ricci-Tersenghi, and J. J. Ruiz-Lorenzo, Phys. Rev. Lett. **103**, 267201 (2009).
[28] L. Leuzzi, G. Parisi, F. Ricci-Tersenghi, and J. J. Ruiz-Lorenzo, Philos. Mag. **91**, 1917 (2011).
[29] R. A. Baños, A. Cruz, L. A. Fernandez, J. M. Gil-Narvion, A. Gordillo-Guerrero, M. Guidetti, D. Iñiguez, A. Maiorano, E. Marinari, V. Martin-Mayor, et al., Proc. Natl. Acad. Sci. U.S.A. **109**, 6452 (2012).
[30] D. Larson, H. G. Katzgraber, M. A. Moore, and A. P. Young, Phys. Rev. B **87**, 024414 (2013).
[31] M. J. Stephen and A. Aharony, J. Phys. C **14**, 1665 (1981).
[32] J. Snider and C. C. Yu, Phys. Rev. B **72**, 214203 (2005).

[33] M. Schechter, P. C. E. Stamp, and N. Laflorencie, J. Phys. Condens. Matter **19**, 145218 (2007).

[34] The single-spin time-reversed state is not involved in this process [7].

[35] K. Binder and A. P. Young, Rev. Mod. Phys. **58**, 801 (1986).

[36] Our results remain unchanged if dipolar interactions in a random system are used, and when short-range exchange interactions are included as is the case for $\mathrm{LiHo_xY_{1-x}F_4}$.

[37] A. K. Hartmann, Phys. Rev. E **59**, 84 (1999).

[38] B. Ahrens, J. Xiao, A. K. Hartmann, and H. G. Katzgraber (2013), (arXiv:cond-mat/1302.2480), 1302.2480.

[39] D. M. Silevitch (private communication).

[40] P. B. Chakraborty, P. Henelius, H. Kjønsberg, A. W. Sandvik, and S. M. Girvin, Phys. Rev. B **70**, 144411 (2004).

[41] A. Biltmo and P. Helenius, Europhys. Lett. **87**, 27007 (2009).

[42] K.-M. Tam and M. J. P. Gingras, Phys. Rev. Lett. **103**, 087202 (2009).

[43] A. Biltmo and P. Henelius, Phys. Rev. B **76**, 054423 (2007).

[44] All estimates of T_c and values of h are in kelvin (K).

[45] Z. Wang and C. Holm, J. Chem. Phys. **115**, 6351 (2001).

[46] G. Mennenga, L. J. de Jongh, and W. J. Huiskamp, J. Magn. Magn. Mater. **44**, 59 (1984).

[47] S. Boettcher and A. G. Percus, Phys. Rev. Lett. **86**, 5211 (2001).

[48] A. A. Middleton, Phys. Rev. E **69**, 055701(R) (2004).

[49] See Supplemental Material for a list of all simulation parameters for both zero- and finite-temperature simulations, as well as a list of all critical parameters determined using a finite-size scaling.

[50] K. Hukushima and K. Nemoto, J. Phys. Soc. Jpn. **65**, 1604 (1996).

[51] H. G. Ballesteros, A. Cruz, L. A. Fernandez, V. Martin-Mayor, J. Pech, J. J. Ruiz-Lorenzo, A. Tarancon, P. Tellez, C. L. Ullod, and C. Ungil, Phys. Rev. B **62**, 14237 (2000).

[52] H. G. Katzgraber, M. Körner, and A. P. Young, Phys. Rev. B **73**, 224432 (2006).

[53] W. H. Press, S. A. Teukolsky, W. T. Vetterling, and B. P. Flannery, *Numerical Recipes in C* (Cambridge University Press, Cambridge, England, 1995).

[54] D. H. Reich, B. Ellman, J. Yang, T. F. Rosenbaum, G. Aeppli, and D. P. Belanger, Phys. Rev. B **42**, 4631 (1990).

[55] Note that a reentrance to a spin-glass phase is a common effect found in glassy spin systems [59, 60].

[56] W. Wu, D. Bitko, T. F. Rosenbaum, and G. Aeppli, Phys. Rev. Lett. **71**, 1919 (1993).

[57] We have performed simulations of a vanilla three-dimensional ferromagnet with bond disorder coupled to a random field. Keeping the strength of the random fields fixed, as well as the ferromagnetic mean of the interactions, we change the width of the Gaussian-distributed bonds around the ferromagnetic mean. Preliminary results qualitatively agree very well with our proposed disordering mechanism and illustrate its generality.

[58] M. J. P. Gingras and P. Henelius, J. Phys.: Conf. Ser. **320**, 012001 (2011).

[59] C. K. Thomas and H. G. Katzgraber, Phys. Rev. E **84**, 040101(R) (2011).

[60] G. Ceccarelli, A. Pelissetto, and E. Vicari, Phys. Rev. B **84**, 134202 (2011).

Supplementary Material: Andresen *et al.*

TABLE I: Simulation parameters for $T = 0$: System of size $L = 6$, 8, and 10, field h and dilution x are studied. $x_{\min}$ [$x_{\max}$] is the smallest [largest] concentration studied and Δx is the step size between measurements. N_{sa} is the number of disorder realizations.

h	$x_{\min}$	$x_{\max}$	Δx	N_{sa}
0.000	0.280	0.350	0.010	5000
0.025	0.275	0.400	0.025	3000
0.050	0.300	0.400	0.025	3000
0.075	0.300	0.600	0.050	1500
0.100	0.400	0.800	0.100	1500

TABLE II: Simulation parameters at finite temperature and $x = 0.32$ for different fields h and system sizes L. The equilibration/measurement times are 2^b Monte Carlo sweeps. $T_{\min}$ [$T_{\max}$] is the lowest [highest] temperature used and N_T is the number of temperatures. N_{sa} is the number of disorder realizations.

x	h	L	b	$T_{\min}$	$T_{\max}$	N_T	N_{sa}
0.32	0.000	6	15	0.100	0.500	25	2000
0.32	0.000	8	17	0.100	0.500	25	2000
0.32	0.000	10	18	0.168	0.500	20	1000
0.32	0.000	12	18	0.240	0.500	15	1000
0.32	0.000	14	16	0.275	0.500	10	750
0.32	0.000	16	16	0.275	0.500	10	385
0.32	0.005	6	12	0.280	0.550	20	2000
0.32	0.005	8	13	0.280	0.550	20	3500
0.32	0.005	10	15	0.280	0.550	20	2000
0.32	0.005	12	17	0.280	0.550	20	1200
0.32	0.005	14	16	0.312	0.550	17	1200
0.32	0.010	6	15	0.050	0.500	30	1500
0.32	0.010	8	17	0.050	0.500	30	1100
0.32	0.010	10	18	0.230	0.500	15	1000
0.32	0.010	12	19	0.245	0.500	15	850
0.32	0.010	14	17	0.265	0.500	15	750
0.32	0.020	6	15	0.050	0.500	30	1500
0.32	0.020	8	18	0.050	0.500	30	1000
0.32	0.020	10	16	0.245	0.500	15	1000
0.32	0.020	12	19	0.245	0.500	15	600
0.32	0.020	14	17	0.274	0.500	13	7500
0.32	0.030	6	14	0.226	0.450	14	3000
0.32	0.030	8	17	0.212	0.450	15	2000
0.32	0.030	10	17	0.226	0.450	14	2000
0.32	0.030	12	19	0.226	0.450	14	600
0.32	0.035	6	13	0.218	0.450	20	3000
0.32	0.035	8	14	0.218	0.450	20	2000
0.32	0.035	10	15	0.218	0.450	20	2000
0.32	0.035	12	18	0.218	0.450	20	650
0.32	0.040	6	14	0.218	0.450	20	3000
0.32	0.040	8	16	0.218	0.450	20	2800
0.32	0.040	10	17	0.218	0.450	20	2000
0.32	0.040	12	17	0.218	0.450	14	1000
0.32	0.050	6	13	0.105	0.500	20	1500
0.32	0.050	8	16	0.150	0.500	20	1000
0.32	0.050	10	18	0.150	0.500	20	1000
0.32	0.050	12	19	0.150	0.500	20	1000
0.32	0.060	6	12	0.150	0.500	20	2000
0.32	0.060	8	16	0.150	0.500	20	2000
0.32	0.060	10	19	0.150	0.500	20	2000
0.32	0.060	12	20	0.150	0.500	20	1000

TABLE III: Simulation parameters at finite temperature and $x = 0.44$. For details see Table II.

x	h	L	b	$T_{\min}$	$T_{\max}$	N_T	$N_{\rm sa}$
0.44	0.000	6	10	0.500	1.000	30	1000
0.44	0.000	8	12	0.500	1.000	30	1300
0.44	0.000	10	13	0.500	1.000	30	2500
0.44	0.000	12	14	0.500	1.000	30	550
0.44	0.000	14	14	0.560	1.000	47	650
0.44	0.020	6	10	0.525	0.800	30	2000
0.44	0.020	8	12	0.525	0.800	30	2000
0.44	0.020	10	13	0.525	0.800	30	1000
0.44	0.020	12	14	0.525	0.800	30	1000
0.44	0.020	14	14	0.550	0.800	30	900
0.44	0.040	6	11	0.525	0.750	22	2000
0.44	0.040	8	12	0.525	0.750	22	2000
0.44	0.040	10	14	0.540	0.750	20	1000
0.44	0.040	12	15	0.550	0.750	20	1000
0.44	0.060	6	11	0.500	0.750	25	2000
0.44	0.060	8	13	0.500	0.750	25	2000
0.44	0.060	10	13	0.519	0.730	19	2000
0.44	0.060	12	14	0.519	0.730	19	1300
0.44	0.080	6	12	0.475	0.725	20	2000
0.44	0.080	8	13	0.475	0.725	20	2000
0.44	0.080	10	13	0.500	0.725	20	1200
0.44	0.080	12	14	0.509	0.725	19	1300
0.44	0.100	6	13	0.445	0.725	23	2000
0.44	0.100	8	14	0.445	0.725	23	2300
0.44	0.100	10	13	0.445	0.725	23	2200
0.44	0.100	12	15	0.475	0.725	20	880
0.44	0.120	6	13	0.425	0.725	30	2500
0.44	0.120	8	14	0.425	0.725	30	2200
0.44	0.120	10	15	0.425	0.725	30	1000
0.44	0.120	12	16	0.445	0.725	25	1000
0.44	0.130	6	13	0.375	0.750	20	2000
0.44	0.130	8	15	0.375	0.750	20	1000
0.44	0.130	10	16	0.375	0.750	20	1000
0.44	0.180	6	14	0.270	0.750	45	3000
0.44	0.180	8	16	0.270	0.750	45	1500
0.44	0.180	10	19	0.270	0.750	45	512
0.44	0.200	6	14	0.270	0.750	45	3000
0.44	0.200	8	16	0.270	0.750	45	2000
0.44	0.200	10	19	0.270	0.750	45	512

TABLE IV: Simulation parameters at finite temperature and $x = 0.65$. For details see Table II.

x	h	L	b	$T_{\min}$	$T_{\max}$	N_T	$N_{\rm sa}$
0.65	0.000	6	10	0.500	1.400	20	1000
0.65	0.000	8	12	0.500	1.400	20	500
0.65	0.000	10	12	0.500	1.400	20	450
0.65	0.000	12	11	0.500	1.400	20	500
0.65	0.000	14	10	0.850	1.400	15	490
0.65	0.000	16	11	0.850	1.400	15	470
0.65	0.050	6	8	0.697	1.400	15	1000
0.65	0.050	8	10	0.697	1.400	15	500
0.65	0.050	10	9	0.800	1.400	20	500
0.65	0.050	12	11	0.697	1.400	15	300
0.65	0.050	14	10	0.900	1.400	15	500
0.65	0.050	16	11	0.920	1.400	16	280
0.65	0.100	6	8	0.820	1.400	20	750
0.65	0.100	8	9	0.820	1.400	20	500
0.65	0.100	10	10	0.820	1.400	20	500
0.65	0.100	12	11	0.820	1.400	20	800
0.65	0.100	14	12	0.820	1.400	20	380
0.65	0.150	6	8	0.820	1.400	20	1000
0.65	0.150	8	10	0.820	1.400	20	500
0.65	0.150	10	11	0.820	1.400	20	500
0.65	0.150	12	12	0.820	1.400	20	500
0.65	0.150	14	13	0.820	1.400	20	500
0.65	0.200	6	10	0.661	1.400	15	500
0.65	0.200	8	11	0.661	1.400	15	400
0.65	0.200	10	14	0.756	1.400	13	1300
0.65	0.200	12	15	0.756	1.400	13	1000
0.65	0.200	14	16	0.756	1.400	13	990
0.65	0.300	6	10	0.600	1.400	20	750
0.65	0.300	8	15	0.600	1.400	20	1000
0.65	0.300	10	17	0.600	1.400	20	550
0.65	0.300	12	19	0.600	1.400	20	530

TABLE V: Critical parameters estimated using a finite-size scaling technique: For each concentration x and field strength h we compute the critical temperature T_c and critical exponent ν.

x	h	T_c	ν
0.32	0.000	0.340(3)	0.83(3)
0.32	0.005	0.335(3)	0.89(3)
0.32	0.010	0.340(3)	0.81(3)
0.32	0.020	0.314(5)	1.04(7)
0.32	0.030	0.281(13)	1.23(17)
0.32	0.035	0.269(14)	1.31(19)
0.32	0.040	0.247(14)	1.41(15)
0.44	0.000	0.584(1)	0.75(1)
0.44	0.020	0.581(1)	0.70(1)
0.44	0.040	0.563(3)	0.77(2)
0.44	0.060	0.548(5)	0.86(3)
0.44	0.080	0.522(5)	0.99(4)
0.44	0.100	0.506(5)	1.01(4)
0.44	0.120	0.466(9)	1.39(12)
0.65	0.000	0.9597(8)	0.79(2)
0.65	0.050	0.9531(10)	0.76(2)
0.65	0.100	0.9264(14)	0.84(3)
0.65	0.150	0.8832(21)	0.91(4)
0.65	0.200	0.8312(41)	1.06(10)
0.65	0.300	0.6905(113)	1.11(12)